

Electron-Stimulated Field Desorption of Multiply Charged Rare-Gas Ions from Tungsten Surfaces

N. Ernst

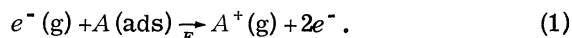
Fritz-Haber-Institut der Max-Planck-Gesellschaft, D-1000 Berlin 33, Germany

(Received 18 August 1980)

By use of field-ion mass spectrometry combined with retarding-potential-energy analysis the experimental evidence for electron-stimulated desorption of field-adsorbed helium and neon atoms as multiply charged positive ions is presented. The abundances of differently charged ions are measured and appearance-energy data are derived from the onsets of integral energy distributions. Within a one-dimensional potential-energy scheme, values for the interaction energy of multiply charged ions with the tungsten substrate are reported.

PACS numbers: 68.45.Da, 79.20.Kz, 79.70.+q

Adding an auxiliary gas of relatively low ionization energy to helium or neon results in the occurrence of higher-energetic lines within the field-ion spectrum of the rare gas. These lines have been observed by using different experimental methods.¹⁻⁴ As proposed by Müller and Krishnaswamy² the appearance of highly energetic rare-gas ions such as ${}^4\text{He}^+$ and ${}^{20}\text{Ne}^+$ may be explained by the impact of electrons with field-adsorbed rare-gas atoms^{5,6} following the reaction



Here, A represents the rare-gas atom which is desorbed after the electron impact as a singly charged ion A^+ by the applied electric field F . The kinetic energy of impinging electrons which are generated by free-space field ionization of the auxiliary gas ranges between several tens and hundreds of electron volts, depending on the applied electric field strength.⁷ Until now only the detection of rare-gas ions which desorb as singly charged species has been reported. In the following, experimental evidence is presented for the electron-stimulated field desorption of multiply charged helium and neon ions from tungsten field emitter surfaces.

The experimental setup, an ultrahigh-vacuum apparatus, consists of a field-ion source combined with a field electron-imaging device, a single focusing magnetic mass spectrometer, and a retarding potential analyzer.⁸ Ions formed at different planes of the emitter crystal (which can be cooled down to liquid-nitrogen temperature) are focused onto the entrance slit of the magnetic mass spectrometer by means of an electrostatic lens and are first analyzed according to their mass-to-charge ratio and are then energy analyzed. The retarder potential can be swept with respect to the emitter potential, and this dif-

ference in potential is fed into the x axis of a multichannel analyzer (MCA). The ion counting rates are registered on the y axis of the MCA simultaneously. Thus, integral energy distributions of differently charged rare-gas ions may be displayed on the cathode-ray screen of the MCA, as presented in Fig. 1. During the experiments hydrogen was mostly used as the auxiliary gas. The kinetic energy of the electrons impinging on the tungsten surface, which under present experimental conditions is covered with field-adsorbed rare-gas atoms,⁹ was determined from the energy distribution of field-ionized hydrogen molecules H_2^+ .⁷ The maximum of the electron energy distribution was measured to be about 450 eV with an energy width at half maximum of about 300 eV for experimental conditions as shown in Fig. 1. The rate of impinging electrons per surface atom was determined by measuring the total electron current reaching the emitter tip and by determining the actual emitter-tip area. It has been estimated that under present experimental conditions the electrons are generated within an ionization zone which is located nearer to the emitter surface than given by the actual value of the emitter-tip radius. Therefore, most of the electrons released by the field ionization of hydrogen should reach the cap of the emitter where the desorption of field-adsorbed rare-gas ions could be initiated. Assuming an effective emission angle of about 120° , one obtains an incoming electron rate of the order of 10^5 e/s per surface atom. Heating effects due to the incoming electron current need not be considered for the present experimental conditions, as discussed elsewhere.⁹ Energy onset curves as shown in Fig. 1 are measured by using a thermally cleaned tungsten tip. They reflect the desorption of ions which are generated at different crystal faces. In the diagrams the two far-right curves display the onset curves of

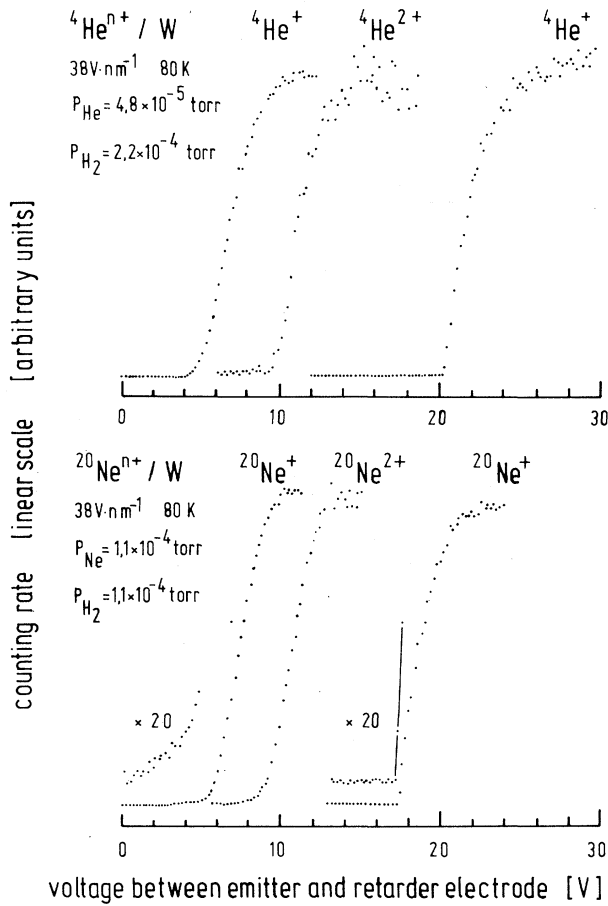


FIG. 1. Energy onset curves of helium and neon ions field emitted from a tungsten tip in the presence of hydrogen gas. The far-right curves within the spectra represent the low-energy deficit part of the integral energy distributions of ordinary field-ionized species. The other curves display integral energy distributions of electron-stimulated field-desorbed ions. Overall field strength values have been derived from Fowler-Nordheim plots of the field-electron current (accuracy $\pm 6 \text{ V nm}^{-1}$) and gas pressures have been measured relatively far away from the tip emitter, which was approximately cooled down to liquid-nitrogen temperature.

field-ionized species, the so-called normal lines of the field-ion energy spectra. For helium, the maxima of the differentiated curves of field-desorbed singly charged species and "normally" field-ionized species ${}^4\text{He}^+$ are found to be separated in energy by 14.9 eV. This number agrees with the value reported previously for electron-stimulated helium desorption from the (111) tungsten surface.¹⁰

Besides the singly charged field-desorbed helium ions, signals with a mass-to-charge ratio of

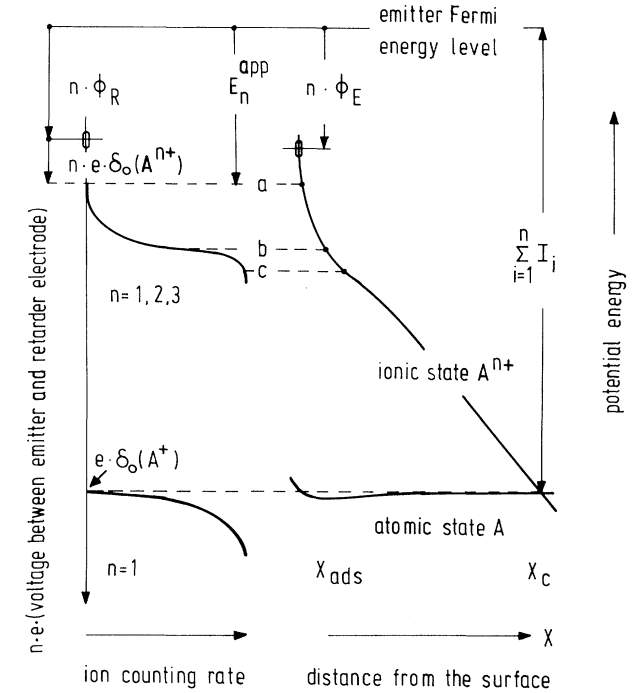


FIG. 2. One-dimensional potential-energy scheme (right-hand side) explaining the electron-stimulated field desorption of multiply charged ions. The lower curve, labeled atomic state, represents the interaction energy of a rare-gas atom with the field-emitter substrate. Atoms which are initially field adsorbed at equilibrium distance x_{ads} may be ionized by electron impact and are strongly accelerated away from the surface as n -fold-charged positive ions by the applied electric field. The potential-energy curve of the ion, labeled ionic state, is bent down because of the presence of the high electric field and crosses the atomic-potential-energy curve at x_c , the critical distance for ordinary field ionization. On the left-hand side of the figure the integral energy distributions of singly charged field-ionized species (lower curve) and electron-stimulated field-desorbed n -fold-charged ions (upper curve) as measured during a retarding-potential experiment are schematically shown. The appearance-energy value of the field-desorbed species, E_n^{app} , as derived from the onset energy $ne\delta_0(A^{n+})$ of the integral energy distribution, is a measure for the interaction energy of multiply charged ions with the substrate atoms with respect to the emitter Fermi energy level. I_i is the i th ionization energy of the atom A ; ϕ_E and ϕ_R are the electron work functions of the emitter and the retarder electrode, respectively.

2 could be detected; these were dependent on the helium gas pressure. The molecular hydrogen ions (which have a mass-to-charge ratio of 2) display minimum energy deficits of about 150 eV under present experimental conditions and may therefore be ruled out as the cause of the third

spectral line. The electron-stimulated field desorption of the ions displaying a mass-to-charge ratio of 2 was also observed using nitrogen as auxiliary gas. This is taken as clear evidence that the newly observed line is indeed representing doubly charged helium ions, ${}^4\text{He}^{2+}$. An interesting feature appearing in the spectra of Fig. 1 is the different shape of the onsets of the integral energy distributions of field-desorbed and field-ionized species. The ion energy distributions of electron-stimulated field-desorbed species display relatively gradual onsets whereas the "normally" field-ionized species show steep onset curves. This is demonstrated in particular for the singly charged neon by magnifying the onset curves by a factor of 20.

The different shapes of the energy onset curves may be explained by use of a potential-energy diagram as discussed in the literature,^{10,11} and which is outlined in Fig. 2. Atomic and ionic potential-energy curves are schematically drawn as a function of distance from the field emitter surface in the right-hand part of the figure. The zero points of the n -fold charged ionic and the neutral atomic state are separated by an amount of energy given approximately by

$$\sum_{i=1}^n I_i - n\varphi_E,$$

with I_i representing the i th ionization energy of the atom A and φ_E being the electron work function of the field-emitter metal. The left side of the figure displays quantities which are measured during retarding-potential analysis of desorbed n -fold charged ions. The lower onset curve represents the low-energy deficit part of the energy distribution of field-ionized species. Under usual field-strength conditions ($20 \text{ V/nm} \leq F \leq 50 \text{ V/nm}$) rare-gas atoms like neon and helium, being in the electronic ground state, may leave the emitter region as singly charged ions at the critical

distance x_c . The appearance-energy value E_1^{app} of field-ionized singly charged species is obtained from the equation

$$E_1^{\text{app}} = e\delta_0(A^+) + \varphi_R, \quad (2)$$

with $e\delta_0(A^+)$ being the onset energy value as derived from the integral energy distribution and φ_R representing the actual value of the work function of the retarder electrode. It has been shown in previous studies^{8,12,13} that appearance-energy data of field-ionized rare gases yield values for the first ionization energy of gaseous atoms which are independent of the applied electric field strength. As shown schematically in Fig. 2, the electron-stimulated field-desorption process is initiated by the electron-impact-induced ionization of an atom A which is initially field-adsorbed at equilibrium distance x_{ads} . Because of the applied electric field, an n -fold charged ion A^{n+} , created at equilibrium distance x_{ads} , is strongly accelerated away from the surface. The traveling time of the slowest ion species ${}^{20}\text{Ne}^+$ for about $3\text{-}\text{\AA}$ distance from the tungsten surface atoms may roughly be estimated to be of the order of 10^{-13} s taking a field strength value of about 40 V/nm . Even if one assumes a local field strength whose value is lower by about one order of magnitude, the estimated traveling times are still more than six orders of magnitude shorter than the average time interval between two electron-impact events at one surface site. Therefore it has to be concluded that multiply charged ions are generated by one-electron-impact processes. Although it is not possible to derive detailed mechanisms for the generation of multiply charged ions from the present experimental results as well as the influence of secondary electrons, which are strongly reaccelerated to the emitter surface, the multiple ionization of adsorbed atoms appears to take place by one-electron-impact events as outlined above and may

TABLE I. Summary of experimental results obtained with conditions shown in Fig. 1.

Desorbed species	Charge number n	Relative abundance (%)	Appearance energy E_n^{app} (eV)
${}^4\text{He}^{n+}$	1	99	8.1
	2	1	25.3
${}^{20}\text{Ne}^{n+}$	1	93	7.4
	2	~6	24.6
	3	~0.03	57

thus be regarded similarly to the multiple ionization of gaseous atoms. An interesting theoretical aspect, which arises from the present observation, is the recombination probability for multiply charged ions in the vicinity of the metal surface. Obviously, the presence of the high electric field reduces the ion neutralization probability in a very drastic manner. The clarification of this point needs more theoretical effort in the basic understanding of electronic properties of highly charged surfaces as represented by a field ion emitter.

The n -fold-charged ion A^{n+} generated at energy level a displays an appearance-energy value given by

$$E_n^{\text{app}} = n[e\delta_0(A^{n+}) + \varphi_R]. \quad (2a)$$

Thus, E_n^{app} data as derived from measured energy-onset curves represent values for the ionic potential energy (with respect to the Fermi energy level) very near to the field-emitter surface atoms.¹⁴ Experimental data for E_n^{app} as well as the observed relative abundances of differently charged field-desorbed ions are summarized in Table I.

The experiments have been performed with the excellent technical assistance of Mr. G. Bozdech. I am grateful to Professor Dr. J. H. Block for stimulating discussions. Financial support by the Deutsche Forschungsgemeinschaft, Bonn Bad

Godesberg, is gratefully acknowledged.

¹A. J. Jason, Phys. Rev. **156**, 266 (1967).

²E. W. Müller and S. V. Krishnaswamy, Surf. Sci. **36**, 29 (1973).

³T. Sakurai and E. W. Müller, Surf. Sci. **49**, 497 (1975).

⁴A. R. Waugh and M. J. Southon, J. Phys. D **9**, 1017 (1976).

⁵T. T. Tsong and E. W. Müller, Phys. Rev. Lett. **25**, 911 (1970), and J. Chem. Phys. **55**, 2884 (1971).

⁶R. G. Forbes and M. K. Wafi, Surf. Sci. **93**, 192 (1980).

⁷T. Sakurai and E. W. Müller, Phys. Rev. Lett. **30**, 532 (1973).

⁸N. Ernst, G. Bozdech, and J. H. Block, Int. J. Mass Spectrom. Ion Phys. **28**, 33 (1978).

⁹N. Ernst, G. Bozdech, and J. H. Block, in Proceedings of the Twenty-Seventh International Field Emission Symposium, The University of Tokyo, 1980, Extended Abstracts (unpublished), p. 151.

¹⁰R. J. Culbertson, T. Sakurai, and G. H. Robertson, Phys. Rev. B **19**, 4427 (1979).

¹¹R. Gomer and L. W. Swanson, J. Chem. Phys. **38**, 1613 (1963).

¹²R. G. Forbes, Surf. Sci. **61**, 221 (1976).

¹³M. Domke, E. Hummel, and J. H. Block, Surf. Sci. **78**, 307 (1978).

¹⁴Possible momentum-transfer processes between incoming electrons and field-adsorbed atoms have not to be taken into account for the discussion of the present experimental results.

Study of the Quadrupolar-Glass Region in Solid D₂ via Proton Magnetic Resonance

W. T. Cochran,^(a) J. R. Gaines, R. P. McCall, P. E. Sokol, and Bruce R. Patton

Department of Physics, The Ohio State University, Columbus, Ohio 43210

(Received 18 June 1980)

Cusplike behavior in the spin-lattice relaxation time of a probe molecule (o -H₂) is used to locate the transition temperature (T_c) to the quadrupolar glass phase of a host o -D₂- p -D₂ alloy for p -D₂ concentrations above 0.29. The values of T_c obtained here are higher than those obtained from line-shape measurements. The spin-echo height is also strongly affected by the collapse of the correlation frequency spectrum near T_c .

PACS numbers: 67.80.Jd, 61.40.Df, 75.50.Kj

Studies of solid hydrogen with use of various NMR techniques¹⁻³ have indicated that, for concentrations of $J=1$ (para) molecules below about $x=0.56$, a rotationally ordered phase can be observed below approximately 0.3 K. Following Sullivan, we will refer to this phase as a quadrupolar glass. Some samples were prepared by ag-

ing high-para-concentration samples in the ordered cubic phase (fcc) and then measuring the splitting of the NMR sidebands¹ as the temperature increased (T_{od}),⁴ whereas others were mixed from the gas components and the measurements of the sideband structure, beats on the free induction decay,^{2,3} and spin-lattice relaxation time (T_1)